Polymer 51 (2010) 5186–5197

Contents lists available at ScienceDirect

Polymer

journal homepage: www.elsevier.com/locate/polymer

Long chain branching polylactide: Structures and properties

Jianye Liu [a], Lijuan Lou [a], Wei Yu [a,*], Ruogu Liao [a], Runming Li [b], Chixing Zhou [a]

[a] Advanced Rheology Institute, Department of Polymer Science and Engineering, Shanghai Jiao Tong University, Shanghai 200240, PR China
[b] College of Chemistry and Chemical Engineering, Henan University, Kaifeng 475004, PR China

ARTICLE INFO

Article history:
Received 11 March 2010
Received in revised form
4 August 2010
Accepted 1 September 2010
Available online 15 September 2010

Keywords:
Polylactide
Long chain branching
Topological structure

ABSTRACT

Long chain branching (LCB) of polylactide (PLA) was successfully prepared by the successive reactions of the end hydroxyl groups of PLA with pyromellitic dianhydride (PMDA) and triglycidyl isocyanurate (TGIC) together. The topological structures of the LCB generated from functional group reactions as well as free radical reactions were investigated thoroughly by gel permeation chromatography (GPC) and rheology. Qualitative information about the branching structures could be readily obtained from linear viscoelasticity, non-linear oscillatory shear experiments and strain hardening in elongational experiments. For quantitative information on chain structure, linear viscoelasticity combined with branch-on-branch (BOB) dynamic model was used to predict exact compositions and chain topologies of the products, which were reasonably explained by the suggested mechanism of functional group reactions. It was found out that the tree-like LCB structure generated in these reactions contributed remarkably to the enhancement of strain hardening under elongational flow, which improves the foaming ability substantially.

1. Introduction

Many studies have focused on the biodegradable polymers over recent decades [1–5] because of their large potential applications in the field of food packaging, biomedical and pharmaceutical use, agricultural films and single-use disposable items. Among them, polylactide (PLA) is one of the most promising choices with relative good mechanical properties and thermal plasticity. Moreover, PLA can be totally produced from renewable agriculture sources. Therefore, the desire for lessening the dependence on petroleum-based materials opens great market opportunities for this environment-friendly polymer.

However, just as most biodegradable polymers, one of the limitations for wide applications of PLA is its poor foamability, for which the main reason is the very low melt strength. During foaming processing, the growth of nuclei and stabilization of cellular structure are strictly related to the melt rheological characteristics, in terms that strain hardening ability should be sufficient to resist the force of bubble growth and then reduce the cell collapse [6]. Many attempts have been made to increase the polymer melt strength, and it is proved that modification of polymers to get branching structures with high molecular weight is an efficient approach to solve this problem [7–9]. It has been widely reported that long chain branching (LCB) had a significant effect on physical properties of polymers, which showed even a small amount of LCB lead to great changes on melt and solution rheological, thermal and mechanical properties [8], as well as the biodegradability of polymers [2]. Branching architectures were reported to increase shrinkage and extension at break of melt-spun PLA fibers, and getting control on these properties by branching is important in the processing of PLA films [9].

Several methods have been tried to obtain PLA with high molecular weight and branching structures. One common method is to have open-ring polymerization of lactides or direct polycondensation of lactic acids, with multifunctional comonomers and catalysts in solution. The catalysts included stannous octoate, tetraphenyl tin [10], $Bi(OAc)_3$ [11] and even lipase enzyme [5]. Several kinds of multifunctional monomers have been used, including multifunctional alcohols [10,11], isocyanates [12], phenyl phoshites [13], epoxies [14]. This way can make the molecular weight increase, however, as it has been reported, chain extending is often more dominant in such systems than LCB [13,15]. For some specific multifunctional monomers, it was found out that manipulating temperature conditions of polymerization at different stages can adjust their reactivity and then lead to the formation of branching structures instead of chain extending [14]. As we have known, extended chains contribute little for the strain hardening behavior. In addition, considering the environment protection, cost, effectiveness, processing convenience and productivity of the preparation, solution reactions are not the best choice. LCB effects can also be introduced by the addition of even low content of poly(D-lactic

* Corresponding author. Tel.: +86 21 54743275; fax: +86 21 54741297.
E-mail address: wyu@sjtu.edu.cn (W. Yu).

0032-3861/$ – see front matter © 2010 Elsevier Ltd. All rights reserved.
doi:10.1016/j.polymer.2010.09.002

acid) (PDLA) to poly(L-lactic acid) (PLLA), in a way that unmelted crystallite acts as a crosslinking point of PLLA chains [16].

The other method is to carry out the branching reactions by reactive processing in bulk, which is evidently more convenient and cheaper, and thus can produce large volume of polymers. The branching reactions can be performed through the functional group reactions or the free radical course. The latter way is very simple and easy to carry out by reactive processing in the presence of some free radical initiators [17]. Branching structures can be introduced, but due to the randomness of free radical branching, it is eventually hard to get control on the molecular weight and topological structure of the final products, which would be proved to have a substantial effect on the foaming properties.

Compared with free radical branching, functional group reactions tend to more easily obtain LCB with "controlled" structures to some extent. However, examples to prepare the LCB of PLA by reactive processing in virtue of functional group reactions have not yet been widely reported. Whereas this approach to get LCB for other polyesters such as poly(ethylene terephthalate) (PET) have been well published [18,19]. By reactive processing in melt, kinds of multifunctional monomers such as epoxy, phenyl phoshites, acid anhydride were used effectively to produce LCB of PET with high molecular weight and high melt strength. It has been published that PLA modified in melt by adding 1,4-butanediol and 1,4-butane diisocyanate together as chain extenders could improve evidently foamability [20]. However, specific components and structures of the product, as well as their relationship with final foaming properties have not yet been clear. Glycidol has been recently tried as a chain extender for PLA in a reactive extrusion process [21], but chain extension is proved to be dominant because chain branching reaction requires higher activation energy and longer reaction time. It is similar as we would find out in this article, that PLA cannot easily get branched using exactly the same approach for PET. However, a two-step functional group reaction has been further developed to realize the branching of PLA in this paper.

The purpose of this paper is to investigate firstly the approach to obtain the highly branched PLA with relatively controlled structures via functional group reactions starting from commercial PLA. Secondly, the LCB products are fully characterized through several methods, not only on the qualitative information on whether the LCB structure exists, but also on the quantitative information on the chain topology, chain length and volume fractions. Finally, this structural information will be correlated with its foaming ability, with guidance on its potential applications in polymeric foam or film.

2. Experimental section

2.1. Materials

The PLA used in this work is a NatureWorks® product 2002D, whose specific gravity and melt index are 1.24 and 8.74(g/10 min, 210 °C, 2.16 kg), respectively. The content of L-lactide is about 96 wt% and the monomer is less than 0.3 wt%. PLA pellets were dried at 40 °C for 24 h under vacuum before mixing and were stabilized by the addition of 0.5 wt% Irganox 1330 antioxidant from Ciba, Switzerland. Pyromellitic dianhydride (PMDA) and phthalic anhydride (PA) were obtained from Sinopharm Chemical Reagent Co., Ltd, China P. R. Triglycidyl isocyanurate (TGIC) was provided by Huangshan Taida Chemical Company, China P. R. All were used as received without any further treatments. Dicumyl peroxide (DCP) with the half-life time of 12 s at 190 °C, dichloromethane, chloroform and cyclohexane were all purchased from Shanghai Chemicals Factory, China P. R.

2.2. Sample preparation and reactive processing

Modification of the original PLA took place in a Haake Rheocord 90 mixer at 190 °C and 210 °C, in order to observe the effects of temperature on the reaction rate, as well as the structure and molecular weight of final products. At first, the rotational speed was set as 20 rpm, then just after the pellets of PLA (65 g) have totally melted, 0.5 wt% Irganox 1330 were added into each sample as the antioxidants followed by 1 min mixing in order to stabilize the sample during the subsequent long chain branching reactions and rheological measurements. PMDA or PA was added, then after 1 min mixing, TGIC was added into the sample followed by 2 min mixing to make the additives disperse as evenly as possible in PLA melt. Finally, the rotational speed was raised to 60 rpm and was kept until the torque curves reached the steady value. In order to evaluate the effect of LCB produced through the functional group reactions, a comparison with the randomly branching sample, treated by 0.2% DCP under the same processing conditions, was carried out. The detailed processing conditions and the formulations are listed in Table 1, and the corresponding torque and temperature curves are shown in Fig. 1.

2.3. Gel determination and FTIR spectroscopy

After the processing, the reacted samples were treated for further determination of gel content and the characterization of Fourier transform infrared spectroscopy (FTIR). Each sample was cut into small pieces and extracted in a fabric bag with an excess volume of boiling chloroform employing Soxhlet extractor for 24 h. Then the extracted fabric bags were vacuum-dried to a constant weight. According to the weight of the insoluble portion, the gel content of the modified PLA sample can be determined. Except for the sample P-P03-T04-190 with 10.25% gel, no gel was observed for other samples here.

On the other hand, the resulting solution containing the soluble portion was dropped slowly down into acetone, followed by the filtration of polymer precipitates to remove the residue of reactants. Then the resulting modified PLA was washed with cyclohexane three times before drying in a vacuum oven at 40 °C for 48 h. The purified polymer was compressed into films (thickness ≈ 50 μm) at

Table 1
The processing conditions and the formulation for all samples.

Sample Code	1330 (wt%)	PMDA (g)	PA(g)	TGIC(g)	DCP(wt%)	T(°C)	η_0[a](Pa s)
P	0.5	–	–	–	–	190	4.56×10^3
P-P03	0.5	0.3	–	–	–	190	6.34×10^2
P-T04	0.5	–	–	0.4	–	190	2.48×10^3
P-P03-T04-190	0.5	0.3	–	0.4	–	190	4.33×10^5
P-P02-T04	0.5	0.2	–	0.4	–	210	3.06×10^5
P-P03-T04	0.5	0.3	–	0.4	–	210	1.96×10^5
P-P04-T04	0.5	0.4	–	0.4	–	210	2.26×10^4
P-A042-T04	0.5	–	0.42	0.4	–	210	3.25×10^3
P-DCP	0.5	–	–	–	0.2	190	2.82×10^4

[a] The zero-shear viscosities of products were obtained through creep measurement at 180 °C.

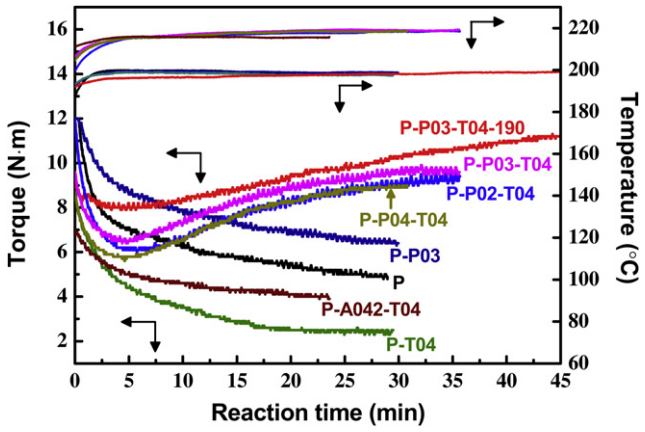

Fig. 1. Torque and temperature evolutions for all PLA sample reaction courses.

180 °C under 12 MPa for FTIR characterization. The FTIR spectra were recorded and analyzed by a Paragon 1000 FTIR spectrometer (PerkineElmer, Inc., USA).

2.4. Gel permeation chromatography

The classical gel permeation chromatography might be incapable of measuring the molecular weight of these branched samples accurately, since the topological structure of the molecule greatly affects the hydrodynamic volume. However, this technique can still supply some important qualitative information on the molecular weight, in order to help us evaluate the branching effect.

Purified samples were dissolved in chloroform at room temperature for 24 h, then injected into SHIMADZU LC solution GPC with chromatograph column Shodex GPC HFIP-806 M at constant 40 °C, with a flow rate of 1.0 ml min^{-1}.

2.5. Rheological measurement

2.5.1. Dynamic shear test

The linear rheological tests were performed on a rotational rheometer (Gemini 200HR, Bohlin Instruments, UK) with parallel plate geometry of 25 mm in diameter and a gap of 0.9 mm. The samples for rheological measurement were obtained by compressing molding into sheet (thickness ≈ 1 mm) at 180 °C under 12 MPa. The stability of samples was checked through the dynamic time sweep test at 1 Hz and 180 °C with the stain amplitude of 1%. The critical strain amplitude for the linear viscoelastic region of pure PLA is about 30% at 1 Hz and 180 °C, and in the range of 10%–18% for other modified samples.

The measurements of small amplitude oscillatory shear (SAOS) were carried out for all samples. Frequency sweeps were performed in the range of 0.01–100 rad s^{-1} with a given strain amplitude of 5%. The zero-viscosity of each sample was obtained by creep experiment at 180 °C with the constant stress of 20 Pa, which was within the linear viscoelastic region of 5200 Pa.

The non-linear oscillatory shear experiments were performed on a strain-controlled ARES G2 rheometer (TA instrument) with parallel plate geometry of 25 mm in diameter and a gap of 1 mm. Tests were performed at 180 °C with the frequency of 0.5 Hz. Both medium amplitude and large amplitude oscillatory shear (MAOS and LAOS) were carried out to evaluate the non-linear dependence of stress response on the strain.

2.5.2. Uniaxial elongation test

The sample sheets were cut into pieces with width of 10 mm and length of 17 mm for the uniaxial elongational viscosity measurements, which were carried out on ARES rheometer (TA instrument) with the extensional viscosity fixture (EVF) at constant strain rates of 0.05, 0.1, 0.3, 0.5 s^{-1} at 160 °C. A pre-elongation for 3 s was performed before the measurements to make sure no slipping between the sample and the fixtures.

2.6. Mechanical properties measurements

An impact test machine Model 2500 from RAY-RAN was used to measure the notched Izod impact strength in conformity to ASTM D256 test standard at room temperature. Sample sheets were cut into ones of 63.5 × 12.7 × 3.18 mm^3 with a V-shape notch of 0.25 mm depth. The hammer swaying velocity was 3.5 m/s.

A tensile machine Instron Model 4465 was used to measure tensile strength in conformity to ASTM D638 test standard at room temperature. The crosshead speed was 50 mm min^{-1}. All mechanical property data were the average value of five repeated tests.

2.7. Foaming by supercritical CO_2

Sample sheets of modified PLA were cut into small sheets of 2 cm × 2 cm and put into a home-made autoclave. Then CO_2 was compressed into the autoclave to the pressure of 13.6 MPa and the autoclave was heated to foaming temperature at 160 °C. After 4 h, the pressure was released at an average speed of about 1.3 MPa s^{-1}. Finally, the products were taken out quickly and put into ice water to freeze the structure of the foams. The foamed samples were fractured in liquid nitrogen, coated with a thin layer of gold on the fracture surface and observed with scanning electron microscope (JEOL JSM-7401F). The accelerating voltage was 5.0 kv.

All the sample preparations and analyses were replicated many times, and the similar results were observed as shown below.

3. Results and discussions

3.1. Reaction evolution

Torque and temperature evolution for all sample reactions are shown in Fig. 1. As the reaction during the addition of reactants is negligible, the moment that rotation speed was changed to 60 rpm is treated as the zero point of reaction time. The real temperature is higher than the set one due to the viscous heating during shear and heat of reactions. The evolution of temperature at a constant setting value is quite similar for different samples, which suggests a similar thermodynamic environment for all the samples with the same setting of temperature, so the effect of temperature on the mechanism or kinetics of reactions is reasonably negligible here. Since the torque value is proportional to the apparent viscosity of materials, which depends on the molecular weight and chain structure of the polymer, the dramatic increase of torque certainly indicates the production of the longer chains or even LCB in reaction system. At first, we would like to get PLA branched by simply reacting with PMDA or TGIC independently, which are the same method used for PET. However, it was out of our expectation that no obvious increase of torque was observed, which should be attributed to the little extending or branching of PLA chains. As shown in Fig. 1, torques of the sample without modification (P) and the sample which independently reacted with PMDA (P-P03) or TGIC (P-T04) decrease monotonously with the mixing time, which is ascribed to the possible thermal degradation of PLA during processing. This phenomenon shows that PLA is quite different from PET in view of long chain branching reaction through functional group reactions. However, the torque shows completely different trend when the sample reacted with these two monomers together.

The torque decreases at first because of possible thermal degradation of polymer, then after less than 5 min, increases monotonously until it reaches a plateau at about 35 min. The increasing torque should be a result of two-step reaction of PLA with PMDA and then TGIC that leads to an increase in the molecular weight and the formation of branching structure. Elevated reaction temperature can effectively reduce the time for the completion of functional group reactions.

In order to make clear the mechanism of the two-step reaction, PA with equal equivalent of acid anhydrides compared with PMDA was used with TGIC under the same processing conditions. The torque curve of P-A042-T04 exhibits the monotonous decrease, indicating no obvious long chain branching reaction occurred in this system but probably only chain extension reaction, which could not suppress the effect of thermal degradation. This result further make us presume that probably two of the three epoxy groups on TGIC reacted in the present two-step reaction, because it would have made P-A042-T04 show the formation of star-like branching structure if all of the three epoxy groups on TGIC react. It seems reasonable if considering the steric hindrance when another carboxyl group on benzene ring (created from anhydride group) reacts with the last epoxy ring on TGIC.

3.2. FTIR spectroscopy

FTIR spectra of original PLA, purified sample P-T04 and P-P02-T04 are shown in Fig. 2, and the dash line guides the peak of transmission at 926 cm^{-1}. It was reported that the epoxide region is around 910–950 cm^{-1} [22], so the peak of transmission at 926 cm^{-1} for sample P-P02-T04 can prove two facts. Firstly, TGIC reacted onto the PLA chains successfully. Secondly, there are epoxy groups left on the PLA chains, which seems to consist of the assumption mentioned above that probably not all the three epoxy groups on TGIC had reacted in the present two-step reaction. However, this peak could not be clearly observed for sample P-T04, which indicates that large amount of TGIC cannot be very easily grafted on PLA chains directly considering the fact that no obvious increase of torque was observed in the reaction system of PLA and TGIC. The number of extended or branched chains should be very low, and such small amount of extended and branched chains cannot compensate the decrease of modulus by degradation, which infers that the rate of reaction for sample P-T04 is rather slow. After the purification of samples, the free TGIC should be washed out and the concentration of the epoxy groups on PLA chains should be too low to detect by FTIR. This different result from the branching reaction of PET might be due to two possible reasons: One is because the reaction activity of terminal carboxyl group on PLA chain is much lower than that on PET chain; the other is because of the low concentration of carboxyl groups on PLA chains, as the terminal carboxyl groups might be end-capped for commercial PLA. We tend to accept the latter reason, so PMDA was chosen to generate the reaction with PLA at the first step.

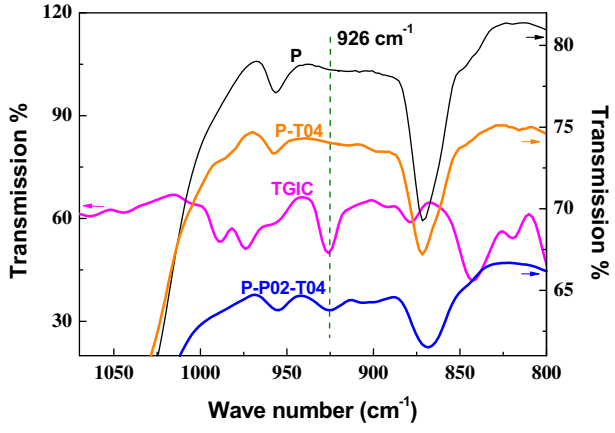

Fig. 2. FTIR spectra (800–1200 cm^{-1}) of TGIC, original PLA, and purified sample P-T04 and P-P02-T04.

3.3. Gel permeation chromatography

Gel determination procedure revealed that only sample P-P03-T04-190 contained 10.25% gel, and no gel was observed for other samples. Molecular weight distribution (MWD) of original PLA and modified samples are shown in Fig. 3. Curves of PLA independently reacted with PMDA or TGIC shifts to the lower molecular weight region possibly due to the thermal degradation. On the contrary, an evident shoulder can be seen at high molecular weight position for all other samples prepared by reacting with PMDA and TGIC together. In our case, this broadening could be interpreted as the result of the presence of LCB of PLA. The similar behavior is also observed for LCB polypropylene made by reactive processing [23]. Although the measured molecular weight and its distribution values are not accurate because of the change on hydrodynamic volume for branched samples, we can still get some important information here. The molecular weight value at the shoulder position is nearly 8 times of that for original linear PLA chain, which indicates the possible formation of LCB chains connecting at least 8 linear chains. Since simply reacting with TGIC or PMDA cannot get such a large molecular weight LCB, this suggests it should be a more complex branching structure that is produced by reacting with the two monomers together. The structure might be similar to the tree-like or other complex topology. By peak separation analysis for branched samples, it is found out that the area of high molecular weight shoulder is about 12% of the whole area under the curve, which can be approximately considered as the content of LCB in the modified sample. However, the GPC curves for P-P02-T04, P-P03-T04 and P-P04-T04 nearly overlap with one another, so the formula effect cannot be evaluated here due to the subtle differences in these GPC results.

3.4. Linear rheology

The dynamic time sweeps of all samples are shown in Fig. 4, from which the stability of the materials can be readily examined. Obviously, the rheological time sweep data can supply more information than the torque curves in Haake batch mixer. The monotonous decreasing viscosity of sample P-P03 indicates only

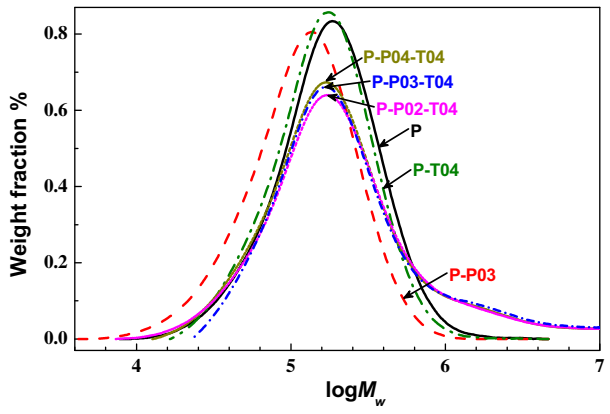

Fig. 3. Molecular weight distributions of original PLA and modified samples.

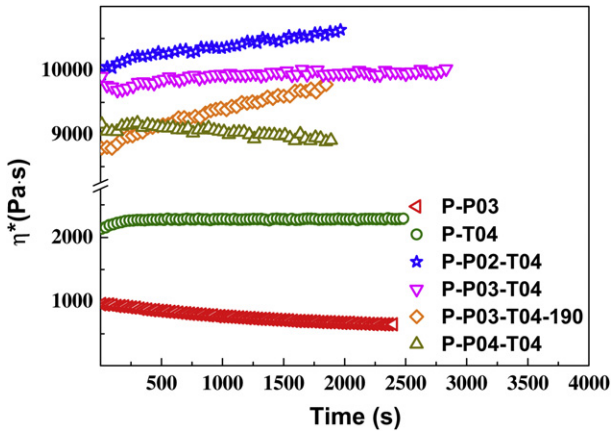

Fig. 4. Dynamic time sweeps of modified samples at 180 °C.

occurrence of degradation, while slight increase of viscosity for P-T04 within the first 200 s reveals the occurrence of chain-extending reaction. The continuous increasing viscosity of sample P-P02-T04 and P-P03-T04-190 suggests the incomplete reaction during processing for producing LCB. To get a reliable data on further rheological test, these samples were annealed under elevated temperature of 210 °C for no more than 1 h to complete the reactions.

Complex shear modulus obtained from frequency sweeps and creep testes of original PLA and modified samples are shown in Fig. 5. The dynamic mechanical spectrum covering 7 magnitudes of angular frequency is the combination of three parts: (i) data in the range of 10^{-2}–10^{2} obtained directly from the frequency sweep; (ii) the terminal region of dynamic modulus (which means $G' \propto \omega^2$ and $G'' \propto \omega$) calculated from the equations (1) and (2) by using data obtained from creep tests [24]; and (iii) the transition region between the two parts above converted from creep data by software TA Orchestrator(version V7.2.0.4). As shown in the figure, these three parts connect well with one another and show clearly different relaxation information of samples.

$$G' = \frac{\omega^2 \eta_0^2 J_e^0}{1 + \left(\omega \eta_0 J_e^0\right)^2} \tag{1}$$

$$G'' = \frac{\omega \eta_0}{1 + \left(\omega \eta_0 J_e^0\right)^2} \tag{2}$$

where η_0 and J_e^0 are the zero-viscosity and steady state compliance, respectively.

Compared with loss modulus, storage modulus can supply more information on possible component of products. The original PLA easily presents terminal region at relatively high frequency, which suggests that the relaxation process of chains is relatively fast and this is the typical behavior of linear polymer. It can be clearly seen that sample P-P03 has smaller modulus compared with the original PLA, most probably due to the thermal degradation during processing. Polymer chains in P-P03 are still almost linear since there is no obvious transition in dynamic modulus at low frequency. P-T04 shows slight different behavior with a relaxation process at lower frequency, indicating a relatively long relaxation process, probably related to the formation of extended chains or even LCB during reaction. According to the lower modulus of P-T04 than that of original PLA at high frequency, it is clear that this increase of modulus due to possible small amount of extended and branched chain cannot compensate the decrease of modulus by degradation.

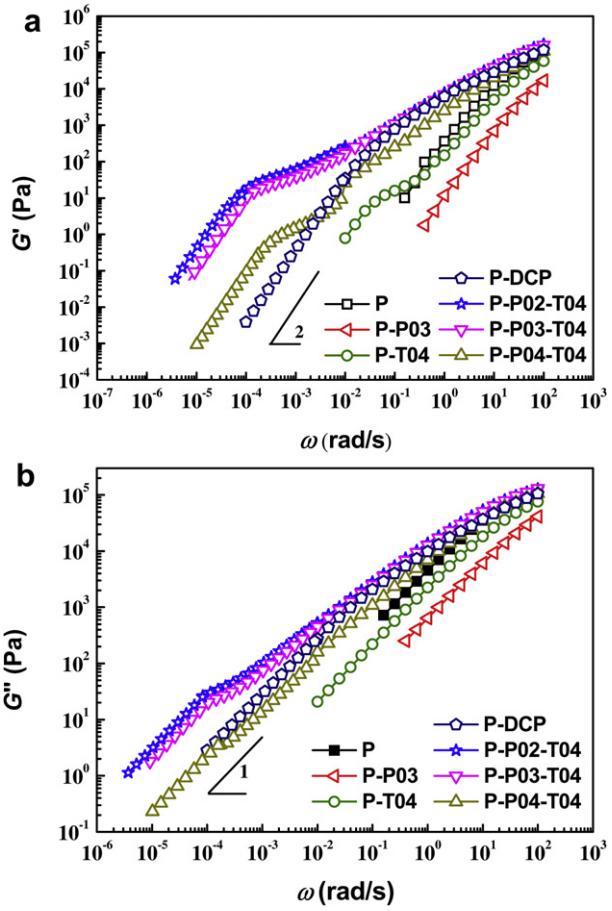

Fig. 5. Dynamic mechanical spectra of PLA samples at 180 °C obtained from frequency sweeps and creep tests: (a) storage modulusG' and (b) loss modulusG''as a function of angle frequency.

This consists with the analysis from the FTIR result that TGIC can react with PLA chain directly more or less but with a rather slow rate of reaction. The dynamic mechanical spectra of three samples modified by using PMDA and TGIC together are evidently different. The transition of storage modulus at very low frequency indicates the appearance of some much longer relaxation time than linear ones, which proves the existence of LCB. Their storage modulus is so much higher than linear ones that only simple star and linear structures cannot result in such a pronounced increase on elasticity of material. Therefore, this phenomenon suggests the generated LCB should have more complex topological structures, quite possibly containing branch-on-branch structures such as tree or comb. The gel in sample P-P03-T04-190 can also prove the existence of these branch-on-branch structures. For different formulations, the occurrence of transition at the same range of frequency indicates the similar types of LCB structures in these products, while their different increase amplitudes of storage modulus suggest the possible dependence of amounts of LCB on the formulations. P-P02-T04 presents the highest storage modulus of the three, indicating its highest molecular weight and LCB degree. P-DCP presents an evidently larger storage modulus and longer relaxation time compared with linear PLA, indicating the presence of randomly branched LCB. In addition, a comparison between P-P04-T04 and P-DCP shows that P-DCP has a larger storage modulus at low frequency and a much faster terminal relaxation. From this result we speculate that P-DCP has relatively larger amount of LCB, but these LCB relax faster than the branched chains in P-P04-T04.

The difference in chain topology can also be illustrated by vGP plot, firstly proposed by van Gurp and Palme [25] to check validity of time and temperature superposition rule. By plotting phase angle vs. complex modulus, vGP plot was proved to be a more transparent way to show the correlation between rheological data with LCB features [26]. As shown in Fig.6, curves of the original PLA and P-P03 are in a typical shape for linear polymer, i.e., the phase angle decreases monotonically without any kinds of transitions with the complex modulus when $|G^*|$ is smaller than the plateau modulus. The existence of small amount of LCB in P-T04 is more evident in vGP plot. The appearance of transition point even at high phase angle shows the generation of other kind of component with longer relaxation time than linear chains. However, such transition should not be ascribed to the bimodal distribution of molecular weight in linear polymer system according to the GPC result for P-T04 mentioned above. The plots for samples prepared with PMDA and TGIC together are intriguing. The evident sharp bump at low phase angle shows clearly the existence of LCB with especially slow relaxation. It was known from literatures that by increasing the level of LCB, vGP plot shifts to the position of lower phase angle [26–28]. The lower phase angle indicates stronger elasticity of materials. Therefore, it can be seen that P-P02-T04 has the highest LCB degree and relatively small amount of LCB with similar structures as those in P-P04-T04. The shape of P-DCP curve confirms the creation of LCB in product, but the relaxation processes of LCB are faster than those in P-P04-T04.

3.5. Nonlinear rheology

To further distinguish the differences in topological structure of three branched samples (P-P02-T04, P-P03-T04 and P-P04-T04), we extend the dynamic experiments to the non-linear region. When the strain amplitude is larger than some critical value, the amplitude of stress response will not be proportional to the strain amplitude and the stress signal is not sinusoidal any more. Usually these non-linear behaviors can be analyzed by Fourier Transform Rheology (FTR) [29–31], although other methods are also possible [32]. Nonlinear oscillatory shear is found to be very sensitive to polymer architectures including molecular weight and molecular weight distribution, the number of arms and their lengths [30]. The FTR converts the stress data in the time domain into frequency dependent spectra, which is even very sensitive to weak signals of high harmonics. As other higher harmonic intensity is often too feeble to be concerned, we usually focus only on the third or fifth complex harmonic of stress (σ_3^* and σ_5^*). If only the third harmonic is considered, the stress $\sigma(t)$ can be expressed as:

$$\sigma(t) = \sigma_1 \sin(\omega t + \varphi_1) + \sigma_3 \sin(3\omega t + \varphi_3) \quad (3)$$

where σ_3 and φ_3 denote the magnitude and phase angle of the third complex harmonic of stress, respectively. Correspondingly, σ_1 and φ_1 represent the magnitude and phase angle of the fundamental frequency. Then the relative intensity of stress (σ_3/σ_1) can be chosen as parameters to characterize the non-linear effect in the periodic stress curve [29–31]. Nonlinear region can be usually divided into MAOS (medium amplitudes oscillatory shear) and LAOS (large amplitudes oscillatory shear). It has been reported [33] that under MAOS (20–120% in our case), the slope of $\log\sigma_3/\sigma_1 \sim \log\gamma_0$ plot was only related to the topological molecular structure of polymer, regardless of molecular weight, molecular weight distribution and test conditions such as excitation frequency and temperature. Moreover, the studies reveal that the slope remains as "2" for linear polymers in the MAOS region and becomes smaller than 2 as the branched level increases [33]. Theoretically, it has been shown that $\sigma_3/\sigma_1 \propto D_e\gamma_0^2$ when the oscillatory shear is just out of linear region [32] for linear polymers, where D_e is the Deborah number, defined as the product of the terminal relaxation time and angular frequency. Therefore, it is suggested that the deviation from 2 can be correlated to the degree of LCB [33], and this slope can be used as a sensitive indicator of LCB level. As shown in Fig. 7, the slope for original PLA is 1.98, which is consistent with the reported studies for linear polymers with this slope of 2. Such slope for branched sample becomes smaller than 2, which ranges from 1.51 to 1.86, indicating the presence of LCB in modified sample. The lowest slope value for the sample P-P03-T04-190 shows its highest degree of LCB among these products, which agrees with the analysis that P-P03-T04-190 is the only sample with a small amount of gel. The formula effect on the final structure leads to conclude that the less amount of PMDA results in higher degree of LCB in products, and this should be explained by the reaction mechanism proposed latter. The structural difference of branched samples can be more evidently characterized under LAOS (150–450%). Higher intensity of nonlinearity indicates higher LCB level in samples, which is consistent with the results got from the slope values under MAOS. Although this is consistent with the previous work on branched PP and PLA [33], it does not agree with the predictions by constitutive equations such as Pom–Pom model, which shows $\sigma_3/\sigma_1 \propto \gamma_0^2$ even for branched molecules [33]. Actually, a non-linear factor can be defined as $Q \equiv (\sigma_3/\sigma_1)/\gamma_0^2$, which should

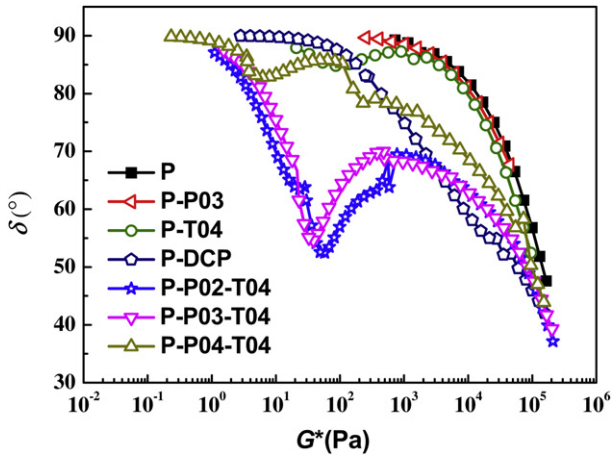

Fig. 6. vGP plots for original PLA and modified samples at 180 °C.

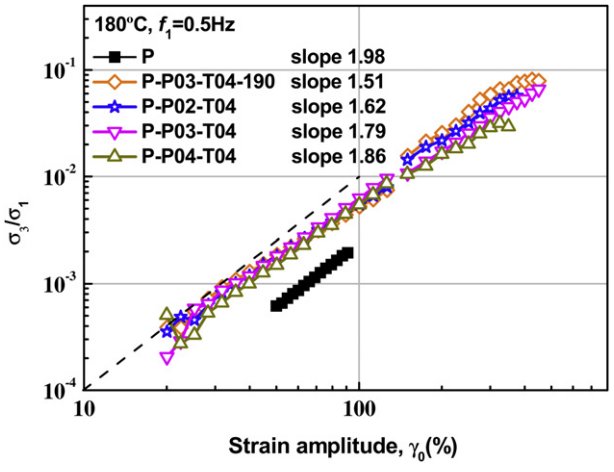

Fig. 7. The relative third stress intensities (σ_3/σ_1) of original PLA and modified samples as a function of strain amplitude (20–450%).

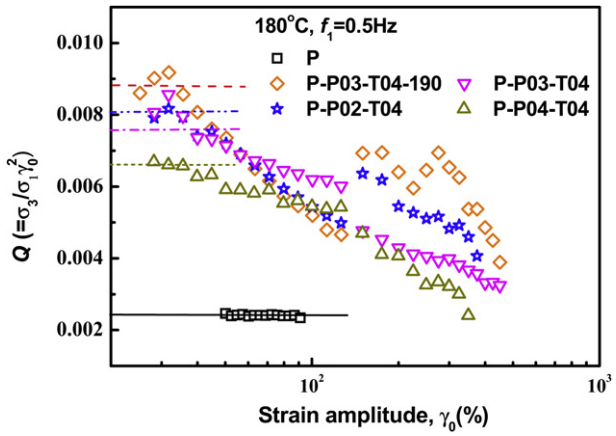

Fig. 8. Coefficient Q as a function of strain amplitude (20–450%) evaluated from the non-linear rheological data for original PLA and modified samples.

be independent of strain amplitude at low strains for linear polymers [34]. Q as a function of strain amplitude is shown in Fig. 8. It is clear that Q is a constant for linear PLA in a wide range of strain amplitude. For branched polymers, the non-linear factors approach constants at low strain amplitude and start to decrease as the strain increases. This suggests the slope of $\log\sigma_3/\sigma_1 \sim \log\gamma_0$ in MAOS region should be 2 at low strain amplitude whatever the polymer chain it is, and the difference between linear and branched chains only lies in the dependence of Q on the strain amplitude. This is also consistent with recent findings on model comb polymers [34]. In LAOS region, an overshoot of Q for P-P03-T04-190 is observed, while Q decreases monotonously with strain amplitude for other branched samples. Moreover, the higher Q value is, the higher LCB level is in the samples.

3.6. Proposed mechanism

The results of reaction evolution curve, FTIR and GPC have shown above that PLA cannot easily get branched as PET by reacting independently with TGIC or PMDA, and less stable ester linkage could make it much more easily degrade than PET during processing. This might be because of two possibilities: the low reaction activity or the low concentration of carboxyl groups on these commercial PLA chains. According to the further studies for the samples produced from PLA–PMDA–TGIC reaction system by gel determination and rheology, we can reasonably consider parts of LCB in these samples should be in complex branch-on-branch topological structure, such as tree or comb types. It is more likely to obtain such high branching degree if the terminal carboxyl groups

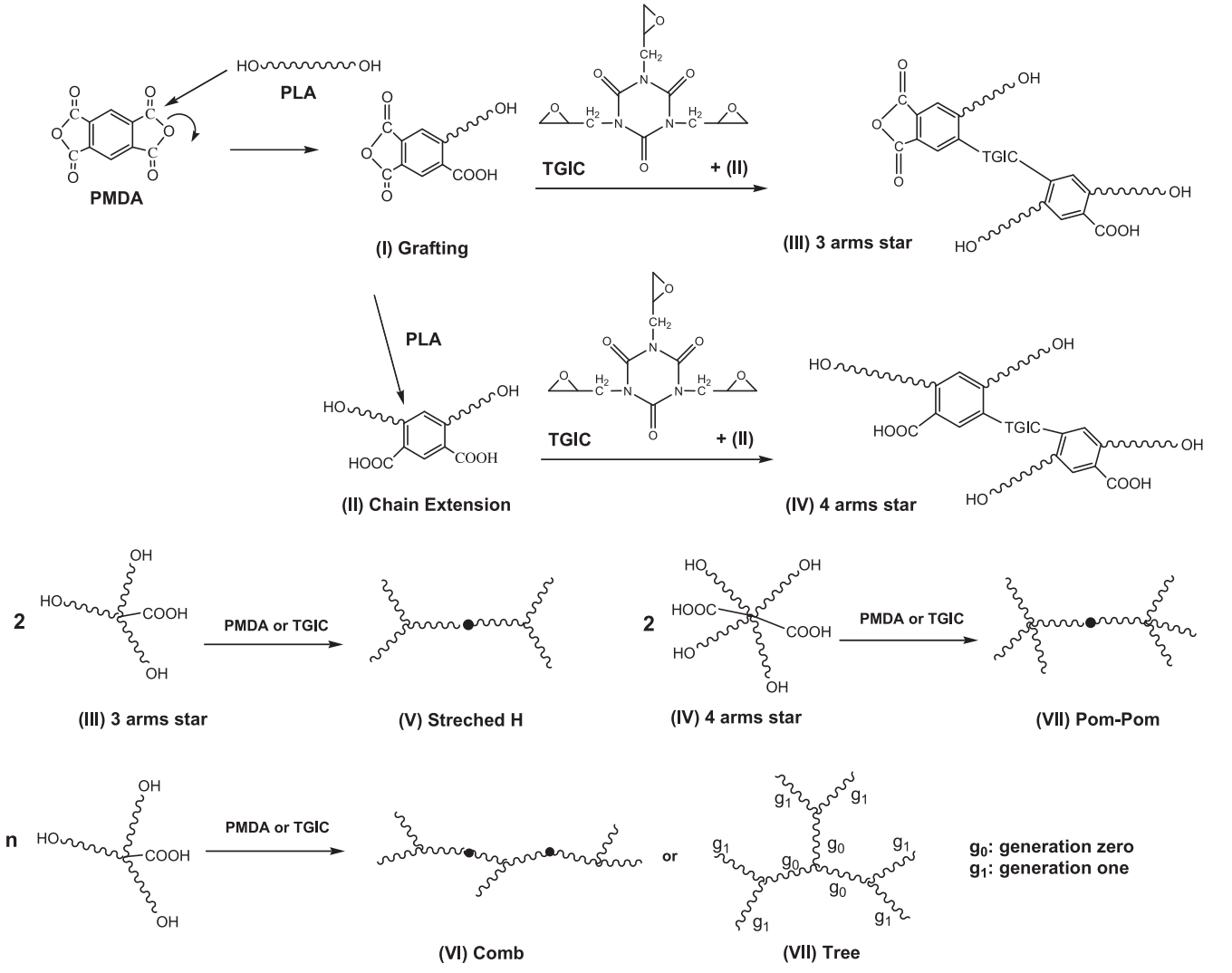

Scheme 1. The two-step reaction sketch and possible chain structures of products.

on PLA chains were end-capped to be hydroxyl groups, which is commonly done for the production of commercial PLA in order to prevent severe degradation for further use. Based on these presumptions, a two-step reaction mechanism is tried to propose in Scheme 1, as well as the corresponding most possible topological chain structure existing in the system.

As shown in Scheme 1, hydroxyl groups at the end of PLA chains open the rings on PMDA and have grafting reaction (I). Then if this reaction is repeated, a chain-extending product (II) can be probably obtained. The carboxyl groups at the end of chain-grafting and chain-extending products may react with two of epoxy groups of TGIC to form star-like PLA (III and IV). Then reactions of hydroxyl and carboxyl groups on star-like chains with PMDA or TGIC possibly bring a large complexity of topological structures of final products, such as stretched H (V), pom–pom (VI), comb (VII) and tree type (VIII). Excessive amount of PMDA would likely cause more grafting reaction and less chain extending and branching, and turn to make the final product more likely to be (I) (in Scheme 1), which contributes less LCB effect. That is why less amount of PMDA led to higher degree of LCB in products. This result is clearly observed in previous study on linear and non-linear rheology: the sample P-P02-T04 has the highest LCB level in the series, and P-P04-T04 is correspondingly slightly branched.

3.7. Proposed chain topology

Although the above rheological measurements suggest formation of LCB, it is still unknown about its exact compositions and chain topology. Actually, this is one of the unsolved problems in molecular characterization of polymers. It is known that the products should be mixtures of several components, each with different chain structures. Typical methods like GPC, light scattering and intrinsic viscosity are almost impossible to be a solution. Rheology, especially linear viscoelasticity, if combined with certain dynamic model of polymer chains, could become an effective approach to the solution. Therefore, accurate constitutive model turns to be important. Fortunately, constitutive model based on molecular dynamics have received much attention recently and a great progress have been made to predict the linear viscoelasticity of polymers with different topological chain structures. The branch-on-branch (BOB) model is one of the most successful models [35]. The basic idea is the hierarchical relaxation of branched structures. With considering the effects of different pathways at different time scales of relaxation process, this model can get dynamic mechanical spectrum by calculating stress relaxation modulus. The relaxation pathways include relaxation faster than the entanglement time, arm-retraction, side arm collapse, retraction of compound arm, reputation and constraint-release rouse motion. By using this general "branch-on-branch" model, linear viscoelasticity of branched polymers with different topological structure can be predicted, including symmetric-star, asymmetric-star, H-type, comb and Cayley tree-like chains. It has been shown that BOB model could predict the linear viscoelasticity of branched chains quite satisfactorily when compared with the experiments of model branched polymers [35]. The details of the model and algorithm will not be repeated here and can be found in the original publication [35].

The BOB model is tried here to find out the compositions and chain structures of different samples, which can be done by fitting the experimental data, i.e., dynamic modulus, phase angle and complex viscosity, with the model predictions. It is required that fitting procedure is successful only when all the data are well matched. The phase angle should be paid more attention due to its much higher sensitivity to the compositions and chain structures than the modulus and viscosity. However, the most difficult thing is how to select the reasonable molecular structures for different

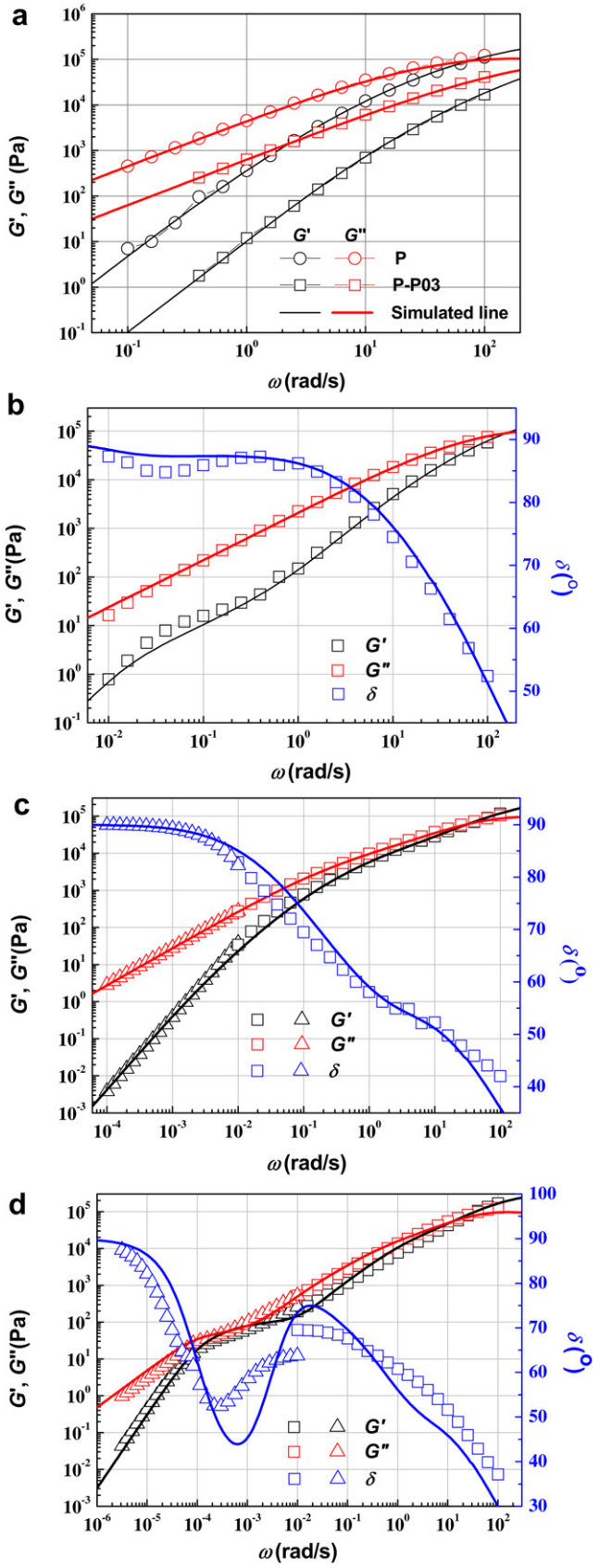

Fig. 9. Linear viscoelastic spectra at 180 °C for (a) P and P-P03; (b) P-T04; (c) P-DCP; (d) P-P02-T04. (square□ is the SAOS data, and triangle△ is the data interpreted from creep test; lines are the results of simulation).

Table 2
Parameters used to fit linear viscoelasticity for PLA samples with three components.

	Component I: Linear Chain		Component II: Star-like Chain with 3 arms		Component III: Tree-like Chain with two generations[a]		
	φ[b]	M_w/PDI	φ	M_a/PDI[c]	φ	M_{g_0}/PDI[c]	M_{g_1}/PDI[c]
P	1.00	120/1.2	–	–	–	–	–
P-P03	1.00	68/1.25	–	–	–	–	–
P-T04	0.99	95/1.2	0.01	120/1.2(two arms) 90/1.2(one arm)	–	–	–
P-P02-T04	0.60	110/1.2	0.25	110/1.2	0.15	50/1.0	220/1.0
P-P03-T04	0.64	100/1.2	0.21	100/1.2	0.15	50/1.0	200/1.0
P-P04-T04	0.50	85/1.2	0.47	85/1.2	0.03	50/1.0	180/1.0
	Component I: Linear Chain		Component II: Comb-like Chain (q: arm number)				
	φ	M_w/PDI	φ	M_b/PDI[c]	M_a/PDI	q	
P-DCP	0.70	100/1.25	0.30	230/1.2	140/1.2	3	

[a] The topological structure is shown in Scheme 1.
[b] φstands for volume fraction of the corresponding component.
[c] M_a and M_b are the molecular weight of side arm and backbone, respectively; M_{g0} and M_{g1} are the molecular weight of the generation zero and one for tree-like chains, respectively. The unit for all molecular weights listed above is kg mol^{-1}.

compositions. Generally, there is no strict protocol for this, but in our case, mechanism of reaction can serve as a good criteria to select the possible topology of molecules. According to the suggested mechanism in Scheme 1, it is assumed that the samples are composed of linear, star and comb or tree-like molecules. Therefore, the parameters for the molecular structures, such as volume fraction, molecular weight and its distribution, arm length, can be obtained by fitting the experimental data with BOB model. The first try is carried out for the linear PLA, whose molecular weight and molecular weight distribution can accurately be determined independently by GPC. The fitting results for the linear PLA (sample P) are shown in Fig. 9(a) and (b). The weight average molecular weight (M_w) is fitted to be 120 kg mol^{-1} and the polydispersity index (PDI, defined as the ratio between the weight average molecular weight and the number average molecular weight) is 1.2 where the molecular weight distribution is assumed to follow log-normal distribution. The molecular weight and its distribution obtained from fitting linear viscoelasticity are quite close to those measured by GPC. Moreover, the molecular parameters can also be determined from fitting the experimental data for the linear polymer. The density of PLA is 1.24 g cm^{-3}, the number of monomer in one entangled segment is 110, and the entanglement time τ_e is 10^{-5} s. These parameters are characteristic parameters for PLA, and can be used in both linear and branched polymers.

The fitting results of linear viscoelasticity for branched PLA samples are also shown in Fig. 9, and the parameters used to fit the linear viscoelasticity, which reveal the most possible chain topology of samples, are listed in Table 2. The transition points in modulus and phase angle manifest the existence of different relaxation mechanisms, which are directly correlated with the topological structures of molecules. Higher degree of branching make the terminal region move to the lower frequency, indicating a much longer time to get the molecules totally relaxed. It can be seen that P-P02-T04 is the most highly branched and P-T04 is the mildest branched one among all samples. The fitted lines are not exactly the same as the experiments, but quite close to the experimental data. Actually, model predictions are rather close to the experiments for the dynamic modulus, only the positions of local maximum/minimum in the phase angle deviate a little, which could be ascribed to the much more complex structures and compositions in the samples. It is shown that only linear chains exist in P-P03, where chains are degraded heavily. The components of P-T04 include linear and only a few star-like chains with 3 arms. PLA samples react with PMDA and TGIC together are all made of linear, star-like and tree-like chains with two generations, whereas PLA treated with DCP is composed of linear chains and relatively small amount of comb-like chains with only 3 arms. The structures of P-P02-T04 can be reasonably explained from the reaction mechanism shown in Scheme 1. Star-like structure (III and IV) can be easily obtained by chain-grafting with PMDA then reacting with TGIC. Then the stars combined with one another to form the tree-like component (VIII). As the linear viscoelasticity of symmetric-star polymer is independent on the arm number, 3-arm star structure is chosen here for the calculation. With consideration of reaction mechanism of this PLA–PMDA–TGIC system, we found out that these parameters are the most probable choices.

3.8. Uniaxial elongation

As compared to the shear rheology, elongational viscosity is more sensitive to the branched molecular structure. Especially, it shows evident increase in transient elongational viscosity under certain strain, known as the strain hardening behavior which has been reported for branched polypropylene [36,37], low density polyethylene [38,39] and grafted polystyrene [40]. Thus, it is often used as a powerful method to characterize the existence of LCB. Fig. 10 shows the transient elongational viscosities under different

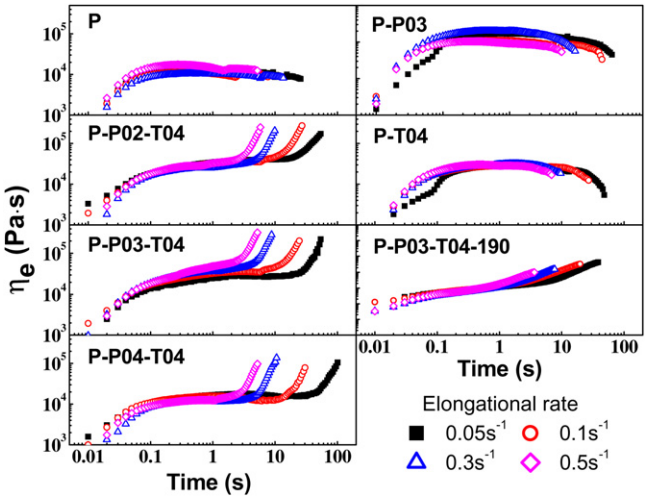

Fig. 10. Elongational viscosity as a function of time at different elongational rates (0.05, 0.1, 0.3, 0.5 s^{-1}) for original PLA and modified samples at 160 °C.

strain rates for all the samples. It is clear that the transient elongational viscosities of original PLA, P-P03 and P-T04 increase with time at the start of stretching, and then decreases, which are called strain softening phenomena. This suggests lack of LCB in these samples. However, it has been shown by linear viscoelasticity that there might be some branched structures in P-T04 sample. Absence of strain hardening in P-T04 sample is ascribed to the requirement on the topological structures of long chain branched molecules. It has been suggested that only branched chain with more than two branching points would show evident strain hardening. In other words, only the stretch of backbone, which is defined as a chain segment with branching points as two ends, can cause strain hardening [27,41]. This implies that the possible branched structures in P-T04 sample could be star-like, which is also consistent with the mechanism of reactions (Scheme 1). However, strain hardening is significant in other samples. The higher strain rate is applied, the earlier strain hardening occurs. As it is also known from literatures that both high molecular weight and high polydispersity can influence the strain hardening behavior [42], it is reasonable to suppose that the high molecular weight tail in GPC result (Fig. 3) for modified sample with PMDA and TGIC is partly responsible for the strain hardening behavior in Fig. 10.

For quantitatively evaluation on the effect of strain hardening behavior, a strain hardening coefficient X_E is defined as $X_E \equiv \eta_E^+(t,\dot{\varepsilon}_0)/3\eta^+(t)$, where $\eta_E^+(t,\dot{\varepsilon}_0)$is elongational viscosity and $\eta^+(t)$is transient shear viscosity in the linear viscoelasticity region [43]. Fig.11 shows the different elongational rate dependence of strain hardening extent for branched samples and P-T04. All X_E values for P-T04 are below 1, showing evident strain softening behavior. Most highly branched P-P03-T04-190 with gel shows a decrease strain hardening with increasing elongational rates, and X_E of highly branched P-P02-T04 as a function of elongational rate runs through a maximum, while strain hardening effects of relatively mildly branched P-P03-T04 and P-P04-T04 increase with higher elongational rates.

It has been shown in literatures that X_E would increase with the elongational rate for polymer with sufficient LCB [36,43], which indicates sample P-P03-T04 and P-P04-T04 have enough entanglements to generate evident strain hardening behavior. Such behavior has been reported for branched polymers with sufficient number of branching points and long enough side arm, including comb-like polystyrene [40] and long chain branched PP [43]. However, completely different trend of X_E is also observed for P-P03-T04-190, which contains about 10% of gel. Such behavior has also been reported but with completely different situations. Investigations on blends of linear PP and LCB-PP [36] have shown that the blends up to 50 wt% LCB-PP showed a decrease of strain hardening with the strain rate, which might be attributed to the insufficient stretch of backbone due to less entanglement of diluted LCB molecules. On the other hand, the study on elongation rheology of PP treated by electron beam irradiation with different doses [43] has also shown a decrease of strain hardening with the elongational rate for sample treated with 20 kGy. The decrease of X_E with the elongational rate is also found for highly branched LCB-PP, which is prepared by reactive processing using peroxide and multifunctional monomers [44]. This is probably because over-crosslinking in gels restricted the stretch on the backbone during elongation. From this point of view, X_E running through a maximum for P-P02-T04 is just a transition between the two as the amount of LCB increases.

3.9. Mechanical properties and melt index

All previous proofs indicate the existence of LCB in prepared samples by using PMDA and TGIC together. Fig. 12 shows the effect of LCB on mechanical properties of material. Compared with the original PLA, the tensile strength of LCB PLA increases quite slightly, while the Izod notched impact strength is well improved by introducing LCB. This increase of impact strength might be related to the change on crystallization by the presence of LCB. Moreover, it can be seen that among our branched samples, higher degree of LCB leads to larger enhance of mechanical properties, but very slight differences in the melt indices of LCB PLA presented in Fig. 12.

3.10. Foaming by supercritical CO_2

The effect of melt strength on foaming processing can be intuitively seen in Fig. 13. The melt strength of original linear PLA is not high enough to keep the foamed structures and no clear cell walls can be observed. Although sample P-DCP has higher melt viscosity compared with the original PLA, it does not show better performance for foaming, either. However, thanks to the tree-like chains in sample P-P02-T04, the melt strength is improved and the structures of foams could be notably well-developed and uniform. The different performance of P-P02-T04 and P-DCP indicates that the foaming property is not only simply related to melt viscosity, but also to the topological structure of polymer chains. From the fitting results as well as the reaction mechanism, it is known that P-P02-T04 has an amount of tree-like chains with two generations, which might most probably be responsible for the much longer time to get completely relaxed and the improvement of foaming

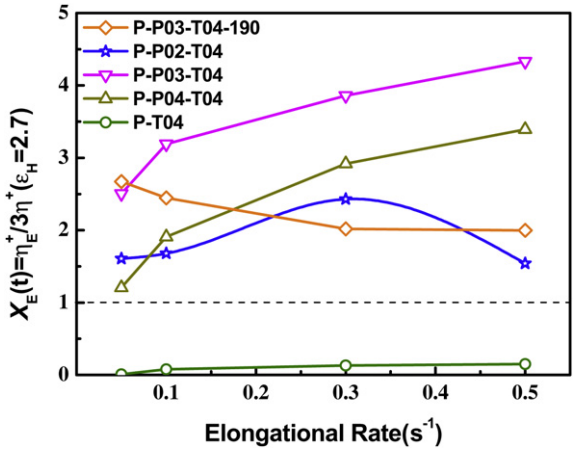

Fig. 11. Strain hardening coefficient X_E under a Hencky strain of 2.7 as a function of elongational rate.

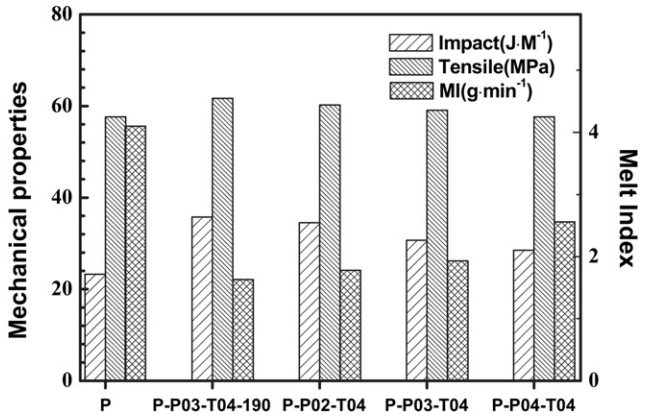

Fig. 12. Mechanical properties and melt indices of original PLA and LCB PLA modified by PMDA and TGIC.

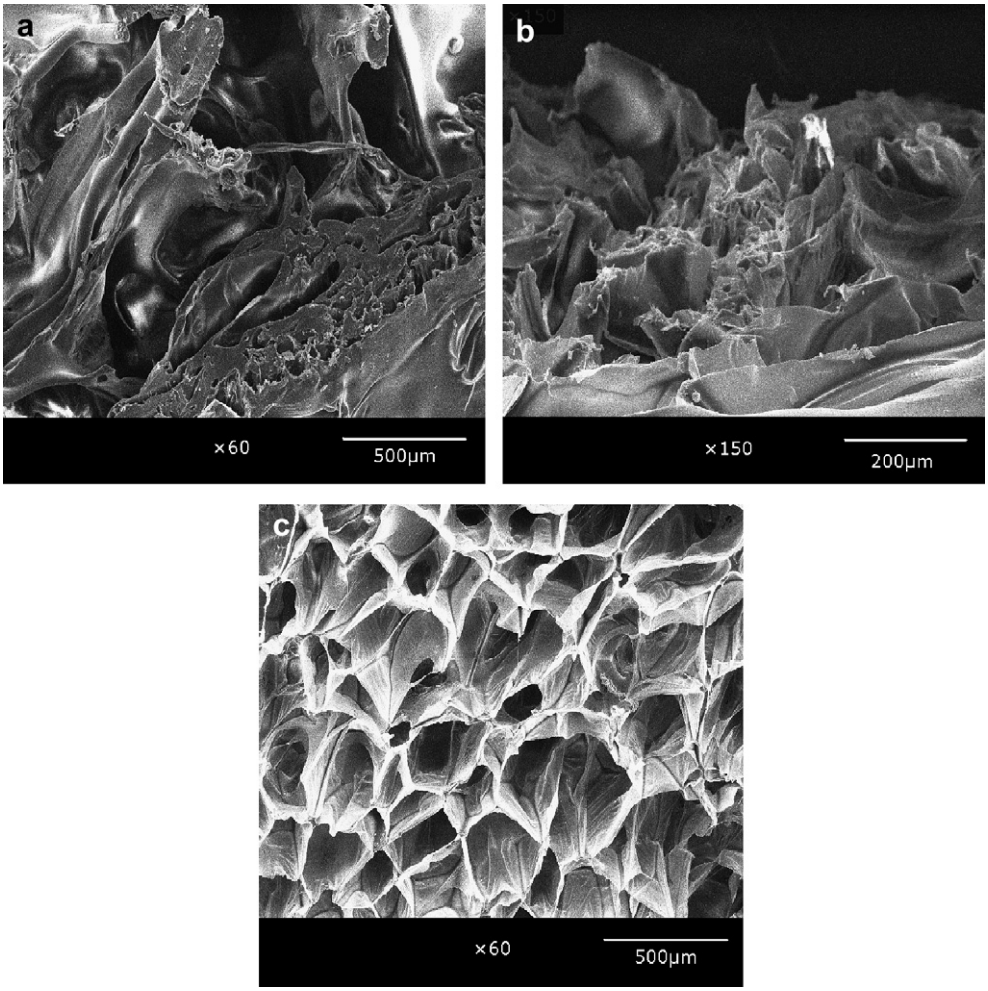

Fig. 13. SEM micrographs of (a) original PLA, (b) P-DCP and (c) P-P02-T04 foams.

performance. On the other hand, the comb chains with only 3 arms in P-DCP do not play an important role for foaming property because of the relatively fast relaxation. Therefore, the branched samples obtained by TGIC and PMDA have better foaming ability than the one obtained by DCP, and such foaming ability is strongly related to the branched chains structures.

4. Conclusions

It is found that the same chain extending or branching strategy for PET fails in the case of PLA, which is possibly due to the low concentration of its end functional group and less stable ester linkage. It has been the first time to find out an approach to get LCB PLA by a two-step functional group reaction with PMDA and then TGIC through reactive processing, in order to try to get an LCB PLA product with relatively "controlled" topological structure to some extent. The appearance of LCB in these products is directly confirmed by FTIR and GPC. Both linear and non-linear rheological results show the generation of some components with much longer relaxation time by this preparation method than those in the randomly branched sample by DCP. Detailed information on exact compositions and chain topological structures of the products were predicted by fitting the linear viscoelasticity to the branch-on-branch (BOB) dynamic model. It is found out that the products of functional reaction are composed of linear, star-like chains with 3 arms and tree-like chains with two generations, while PLA treated with DCP is made of linear chains and small amount of comb-like chains with about 3 arms. All these structures can be reasonably explained by the suggested reaction mechanism. Finally it is proved by strain hardening behavior and foam morphology that the tree-like chains contribute remarkably to foaming properties of the material, in a way that a very long relaxation process generate by many branching points on backbones increase largely the elasticity and melt strength. Therefore, it can be concluded that topological structure of polymer is the substantial factor for the foaming properties.

The temperature and formulation effects on this two-step reaction were also partly investigated. The lower reaction temperature (such as 190 °C) decreases the reaction rate but increases the extent of reaction to induce a formation of gel in system. Within our study range, relatively small amount of PMDA would be helpful to get the product with higher LCB level, which can be reasonably explained by the proposed reaction mechanism.

As the chain topology has a great effect on the final properties of PLA material, getting control on topological structure by reactive processing is meaningful and important. This work is a first try, and much study need to be done in order to get more powerful control on final structure by adjusting the conditions and formulations.

Acknowledgements

This work is financially supported by the Natural Science Foundation of China (NSFC) No. 50390095. and No. 50930002, and

Shanghai Leading Academic Discipline Project (No. B202). W. Yu is supported by the SMC project of Shanghai Jiao Tong University.

References

[1] Chandra R, Rustgi R. Prog Polym Sci 1998;23(7):1273–335.
[2] Tasaka F, Ohya Y, Ouchi T. Macromolecules 2001;34(16):5494–500.
[3] Bordes P, Pollet E, Averous L. Prog Polym Sci 2009;34(2):125–55.
[4] John J, Mani R, Bhattacharya M. J Polym Sci A Polym Chem 2002;40(12):2003–14.
[5] Numata K, Srivastava RK, Finne-Wistrand A, Albertsson AC, Doi Y, Abe H. Biomacromolecules 2007;8(10):3115–25.
[6] Marrazzo C, Di Maio E, Iannace S. J Cell Plast 2007;43(2):123–33.
[7] Gotsis AD, Zeevenhoven BLF, Hogt AH. Polym Eng Sci 2004;44(5):973–82.
[8] McKee MG, Unal S, Wilkes GL, Long TE. Prog Polym Sci 2005;30(5):507–39.
[9] Cicero JA, Dorgan JR, Garrett J, Runt J, Lin JS. J Appl Polym Sci 2002;86(11):2839–46.
[10] Kim SH, Han YK, Kim YH, Hong SI. Makromol Chem 1992;193(7):1623–31.
[11] Kricheldorf HR, Hachmann-Thiessen H, Schwarz G. Biomacromolecules 2004;5(2):492–6.
[12] Woo SI, Kim BO, Jun HS, Chang HN. Polym Bull 1995;35(4):415–21.
[13] Jacques B, Devaux J, Legras R, Nield E. Macromolecules 1996;29(9):3129–38.
[14] Pitet LM, Hait SB, Lanyk TJ, Knauss DM. Macromolecules 2007;40(7):2327–34.
[15] Gu SY, Yang M, Yu T, Ren TB, Ren J. Polym Int 2008;57(8):982–6.
[16] Yamane H, Sasai K, Takano M. J Rheol 2004;48(3):599–609.
[17] Carlson D, Dubois P, Nie L, Narayan R. Polym Eng Sci 1998;38(2):311–21.
[18] Japon S, Boogh Y, Manson JAE. Polymer 2000;41(15):5809–18.
[19] Incarnato L, Scarfato P, Di Maio L, Acierno D. Polymer 2000;41(18):6825–31.
[20] Di YW, Iannace S, Di Maio E, Nicolais L. Macromol Mater Eng 2005;290(11):1083–90.
[21] Deenadayalan E, Lele AK, Balasubramanian M. J Appl Polym Sci 2009;112(3):1391–8.
[22] Dhavalikar R, Xanthos M. Polym Eng Sci 2004;44(3):474–86.
[23] Lagendijk RP, Hogt AH, Buijtenhuijs A, Gotsis AD. Polymer 2001;42(25):10035–43.
[24] Ferry JD. Viscoelastic properties of polymers. New York: Wiley; 1980.
[25] van Gurp M, Palmen J. Rheol Bull 1998;67:5–8.
[26] Trinkle S, Walter P, Friedrich C. Rheol Acta 2002;41(1–2):103–13.
[27] Lohse DJ, Milner ST, Fetters LJ, Xenidou M, Hadjichristidis N, Mendelson RA, et al. Macromolecules 2002;35(8):3066–75.
[28] Barroso VC, Maia JM. Polym Eng Sci 2005;45(7):984–97.
[29] Fleury G, Schlatter G, Muller R. Rheol Acta 2004;44(2):174–87.
[30] Schlatter G, Fleury G, Muller R. Macromolecules 2005;38(15):6492–503.
[31] Vittorias I, Parkinson M, Klimke K. Rheo Acta 2007;46(3):321–40.
[32] Yu W, Wang P, Zhou CX. J Rheol 2009;53(1):215–38.
[33] Hyun K, Baik ES, Ahn KH, Lee SJ, Sugimoto M, Koyama K. J Rheol 2007;51(16):1319–42.
[34] Hyun K, Wilhelm M. Macromolecules 2009;42(1):411–22.
[35] Das C, McLeish TCB. J Rheol 2006;50(2):207–34.
[36] Stange J, Uhl C, Münstedt H. J Rheol 2005;49(5):1059–79.
[37] Auhl D, Stange J, Münstedt H, Krause B, Voigt D, Lederer A, et al. Macromolecules 2004;37(25):9465–72.
[38] Münstedt H, Kurzbeck S, Egersdorfer L. Rheol Acta 1998;37(1):21–9.
[39] Gabriel C, Münstedt H. J Rheol 2003;47(3):619–30.
[40] Hepperle J, Münstedt H. Rheol Acta 2006;45(5):717–27.
[41] Pearson DS, Muller S, Fetters LJ. J Polym Sci Polym Phys Ed 1983;21(11):2287–98.
[42] Münstedt H, Laun HM. Rheol Acta 1981;20(3):211–21.
[43] Krause B, Voigt D, Haubler L, Auhl D, Münstedt H. J Appl Polym Sci 2006;100(4):2770–80.
[44] Tian J, Yu W, Zhou C. Polymer 2006;47(23):7962–9.